J|A|C|S COMMUNICATIONS

Published on Web 02/04/2010

Rigid Pillars and Double Walls in a Porous Metal-Organic Framework: Single-Crystal to Single-Crystal, Controlled Uptake and Release of Iodine and Electrical Conductivity

Ming-Hua Zeng,*[,†] Qiang-Xin Wang,[†] Yan-Xi Tan,[†] Sheng Hu,[†] Hai-Xia Zhao,[‡] La-Sheng Long,[‡] and Mohamedally Kurmoo[§]

Key Laboratory for the Chemistry and Molecular Engineering of Medicinal Resources (Ministry of Education), School of Chemistry & Chemical Engineering, Guangxi Normal University, Guilin 541004, People's Republic of China, State Key Laboratory of Physical Chemistry of Solid Surface and Department of Chemistry College of Chemistry and Chemical Engineering, Xiamen University, Xiamen 361005, People's Republic of China, and Laboratoire de Chimie de Coordination Organique, CNRS-UMR7140, Université de Strasbourg, 4 rue Blaise Pascal, 67000 Strasbourg Cedex, France

Received September 30, 2009; E-mail: zmh@mailbox.gxnu.edu.cn

During the past few years the research on nanoporous metal-organic frameworks (MOFs) has been very fruitful. A large number of frameworks have been synthesized and characterized, and some have shown fascinating gas sorption properties, especially fuel gases.[1] The known MOFs are invariably single-walled and are based on either inorganic single metal centers or clusters or chains connected by organic ligands to form 3D structures.[2] Thus, there is some flexibility in the networks that are sometimes experienced during desolvation. There exist several rigid-pillared MOFs, but there are no double-walled MOFs.[2,3] In this communication, we present a synthetic strategy to create MOFs by employing two different organic connectors: one to generate the rigid metal-organic pillars and the other to make the aromatic walls. For the former we chose lactate anion (DL-lac), which is small and has a high coordination capability due to the peripheral oxygen atoms, and for the latter we chose 4-pyridylbenzoate (pybz), which is long, polar, and ditopic at the opposite ends through the pyridine and the carboxylate. Although we did not anticipate a double-walled MOF, the shape of the pillar, the multiple coordination geometries of the zinc atoms, and the alternate arrangement of the long pybz collectively resulted in the double-walled MOF. Herein, we report the synthesis, crystal structures, and characterization of $\{[Zn_3(DL\text{-}lac)_2(pybz)_2]\cdot 2.5DMF\}_n$ (**1**) and its desolvated form (**1′**). Driven by the recent successful encapsulation of other functional species such as drugs,[4] dyes,[5] light emitters,[6] magnetic molecules,[7] explosives,[8] etc. into the pores, we further explore its gas sorption properties, solvent exchange, kinetics of iodine loading, and release in comparison to zeolite 13X and activated carbon, as well as the electrical conductivity of the iodine-loaded compound ($\mathbf{1'}\supset 3I_2$).

1 was obtained by solvothermal reaction of zinc(II) nitrate, DL-lactic acid and 4-(pyridin-4-yl)benzoic acid in DMF. X-ray crystallography reveals that **1** crystallized in the tetragonal space group $P\bar{4}2_1c$ with an asymmetric unit consisting of one formula unit, and the structure is built around infinite pillars of $\{[Zn_3(DL\text{-}lac)_2]^{2+}\}_n$ (Figure 1a and Figure S1 and Tables S1 and S2 (Supporting Information)).[9] There are three crystallographically independent Zn^{II} atoms with different coordination numbers, 4−6. Zn1 adopts an octahedral coordination with four carboxylate oxygen atoms of two different lactate ligands and the oxygen atom and nitrogen atom of two different pybz ligands. Zn2 is tetrahedral and is bonded to two hydroxyl oxygen atoms and two carboxylate oxygen atoms from two different lactate and pybz ligands, respectively. There is evidence of a pseudosymmetry element in structure **1**, which is a local inversion center on Zn2. Zn3 is analogous to Zn1, but the coordination number is lowered from 6 to 5, owing to the carboxylate group of lactate being reduced from chelate to monodentate. Each lactate ligand in **1** offers two carboxylate oxygen atoms and the deprotonated hydroxyl oxygen to connect three Zn(II) ions within the pillars. The left- and right-handed alternate in a three-center short bridging mode to form $Zn1_4$ or $Zn3_4$ cyclic tetramers which are then bridged by the tetrahedral Zn2. Consequently the pillars are rather rigid through the stable novel Zn_4O_4 SBU. These pillars are then bridged in a square fashion by the pybz spacers with alternate polarity to form the double walls. The presence of pillars and continuous double walls prevent interpenetration of the framework. The DMF molecules are housed in channels with the dimensions 11.2 × 10.2 Å (excluding the van der Waal radii of the surface atoms). Two and a half guest DMF molecules per formula unit are observed in the square channels, as

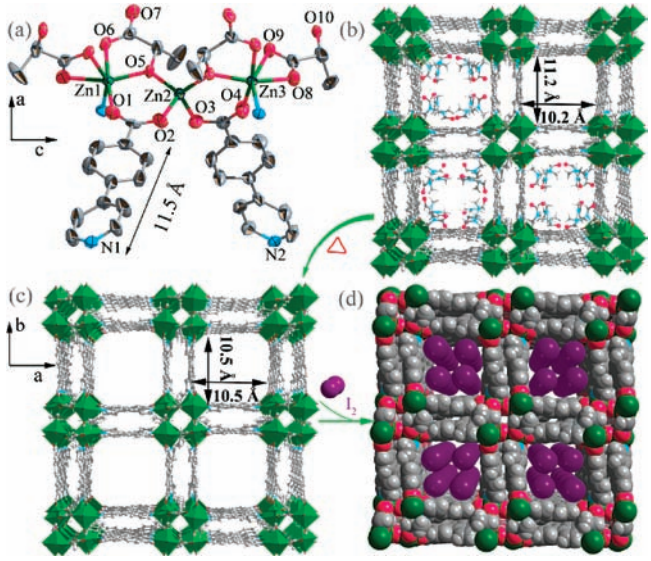

Figure 1. (a) Coordination environment of Zn atoms in **1** (the H atoms are not shown for clarity). (b) Perspective views of the 3D open framework with 1D channel in **1**, the guest DMF molecules being shown in channels. General color code: Zn, green; N, blue; O, red; C, 50% gray; H, 25% gray. (c) The completely desolvated framework of **1′**, showing formal channels. (d) Sketch of I_2 molecules diffusing in the channels of **1′**. The void space in **1** (without guest molecules), calculated by PLATON,[10] is 43.8%.

[†] Guangxi Normal University.
[‡] Xiamen University.
[§] Université de Strasbourg.

established by elemental and thermogravimetric (TG) analyses (Figure S2 (Supporting Information)). It is worth noting that the long bridging pybz ligand has a length of 11.5 Å.

To our surprise, by soaking crystals containing DMF in neat methanol, the latter replaces all the DMF in the crystals. Therefore, there are two ways of obtaining the desolvated crystals of **1′**. One is to heat the as-synthesized DMF containing crystals under vacuum, and the other is to pump on the methanol-loaded crystals.[11] The key features in the structure of **1′** are similar to those found for **1**. All the carboxylate groups of the lactate ligands adopt a monodentate coordination mode linking adjacent Zn^{II} atoms, thus resulting in a slight structural deformation of the framework. The difference in the lattice parameters is due to the equivalence of Zn1 and Zn3 in **1′**, and consequently, the channels adopt a symmetric shape (10.5 × 10.5 Å, Figure 1c). The free volume of **1′** (43.5%) is not much different from that of **1**. The TGA measurements performed on as-synthesized **1** show that the desolvated form **1′** is highly stable up to 400 °C, as shown by variable-temperature powder X-ray diffraction measurements (Figure S3 (Supporting Information)). Such striking thermal stability can be associated with the strong intra- and inter-rod connections. This remarkable feature demonstrates that these types of MOFs may indeed be suitable for applications requiring frequent loading and unloading of guests.[11,12]

The N_2 adsorption isotherm of complex **1′** at 77 K (Figure S4 (Supporting Information)) displays a type I sorption behavior. The apparent surface area was calculated using the Langmuir method to be 918.5 $m^2\ g^{-1}$ (762.5 $m^2\ g^{-1}$ BET), which further confirms the permanent porosity of complex **1′** (Figure S5 (Supporting Information)). Indeed, the results are comparable to those for a recently reported MOF[13] and are better than the highest surface area observed for any known zeolite (zeolite Y, 904 $m^2\ g^{-1}$).[14] These observations imply that the porous structure in **1′**, combining firmness and flexibility, is architecturally suitable for accommodation of some ordered molecules with special directional physical properties.[15] These particular properties thus prompted us to search for absorption properties for other molecules. Given the biological security of zinc and lactate in humans, and the need for iodine in treating hypothyroidism, we successfully loaded the porous crystals with I_2 by suspending the desolvated crystals in a solution of I_2 in cyclohexane. One gram of **1′** can absorb approximately 1 g of iodine.

To explore the uptake and release kinetics of iodine in **1′**, we performed different tests. First we tested if the crystal undergoes dissolution and recrystallization in the cyclohexane solution of iodine by choosing a single crystal and showed that the form and size has not changed during the process but the color has intensified from colorless through yellow and dark brown to black with time (Figure 2a and Figure S6 (Supporting Information)). Second, we tested for the amount of iodine that can be inserted in the pores. We immersed a few samples (100 mg of single crystals) of **1′** in a sufficient amount of a cyclohexane solution of I_2 (0.1 M/L) in a small sealed flask at room temperature, and we observed that the dark brown solutions of I_2 fade slowly to very pale red (Figure 2b), while the crystals of **1′** get darker. Similar behaviors were also observed in aromatic solvent (benzene) with a noticeably slower rate result from the stronger benzene−I_2 interaction (Figure S7 (Supporting Information)). IR, Raman, and XRPD data confirmed the crystallinity of the host framework of the crystal and powder samples of **1**⊃xI_2 (Figures S3, S8, and S9 (Supporting Information)). Most of the peaks in the XRPD remained at similar 2θ positions but were distinctly weakened and broadened. The change of intensity and width indicates that the resulting solid **1**⊃xI_2 retains

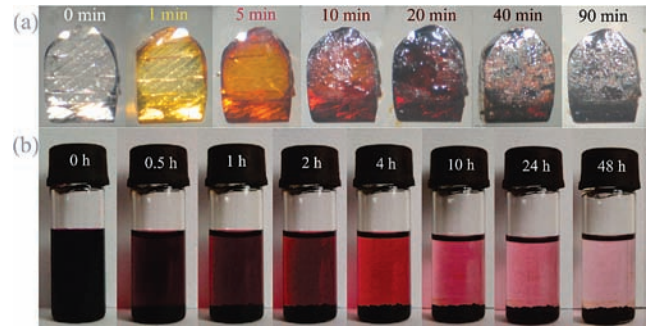

Figure 2. (a) Photographs showing the visual color change when a single crystal of **1′** (0.6 × 0.5 × 0.3 mm^3) was immersed in the cyclohexane solution of I_2 (0.1 M/L). No further change in color and morphology occurred after 90 min. (b) I_2 enrichment progress when 100 mg of crystals of **1′** were soaked in 3 mL of a cyclohexane solution of I_2 (0.1 M/L).

Figure 3. The same weights of different adsorbents (100 mg, using lumps of similar sizes, respectively) immersed in a cyclohexane solution of I_2 (0.1 M/L, 3 mL). The photographs reveal the different inclusion rates and degrees of zeolite 13X and activated carbon in comparison with those of **1′**.

the host framework crystallinity as I_2 molecules diffused in. Although the single crystals retained their original well-defined external forms, the crystals diffract poorly the X-ray beam and the resolution of the structure was poor. On the other hand, we can observe changes in the thiosulfate determination, EA, TGA, and UV/vis spectroscopy (Figures S10−S13 (Supporting Information)). The final mass of crystals of **1′** increases by ca. 100 wt % after being immersed in the cyclohexane solution of I_2, which could be associated with a maximum of 3.02 I_2 being adsorbed per formula unit of **1′**. Thiosulfate determination of the I_2 content released from **1**⊃xI_2 indicates the absorption of 3.03 I_2 for 3 zinc atoms of **1′**. A value of $x \approx 3.03$ in **1′**·xI_2 was also confirmed by EA. Taking into account the coherence and the error of the different techniques above, the reliable included iodine number is $x = 3$. The iodine content is underestimated by UV/vis spectroscopy and TGA, due to the fact that some I_2 remains in the MOFs channels (Table S3 (Supporting Information)). The calculated density of I_2 in **1′**⊃$3I_2$ is estimated to be 2.48 g/cm^3 on the basis of the weight of I_2 and the free volume of **1′**. In comparison, the uptake of I_2 (1.01 g/g) on **1′** is remarkable and clearly exceeds that of zeolite 13X (0.32−0.38 g/g, with 10 Å pore)[16] and activated carbon (∼0.84 g/g) in the cyclohexane solution of I_2 (Figure 3 and Figures S14−S19 (Supporting Information)). The exceptional affinity of **1′** for I_2 may be attributed to the structural character of the regular π-electron walls made of pybz. That is, there is a striking difference compared to conventional adsorbent materials that are lacking an accessible interaction between I_2 and the host. A few examples of I_2 inclusion into organic/inorganic porous frameworks[17] and into MMOFs[18] are known, with the loading weight varying from 16.6% to 82.6%. To the best of our knowledge, such a high I_2 enrichment behavior for **1′**, a metal-organic framework, has never been reported to date.

Conversely, the regular confined nanospace combining abundant π-electron walls may cumulate the advantages to achieve a better-controlled release of I_2, in contrast to conventional adsorbents. The delivery of I_2 from **1′**⊃$3I_2$ performed in ethanol, a nonaromatic

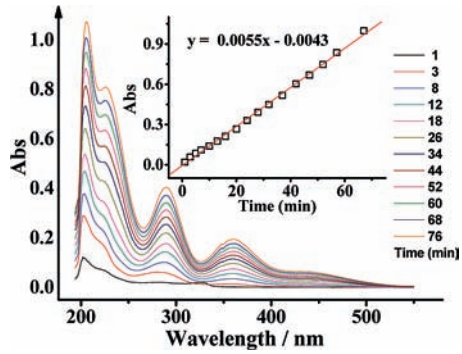

Figure 4. Temporal evolution of UV/vis absorption spectra for the delivery of I_2 from $\mathbf{1}'\supset 3I_2$. Inset: fit curves of the controlled delivery of I_2 ($[I_2] = Kt$) in the first 1 h.

solvent, at room temperature under continuous stirring was determined by UV/vis spectroscopy.

The kinetic of I_2 delivery is empirically adjusted as zero order (Figure 4 and Figures S15 and S16 (Supporting Information)). The delivery of I_2 in ethanol increases linearly with time, indicating that the I_2 release is governed by the host−guest interaction. The release rate of the $\mathbf{1}'\supset 3I_2$ crystal was estimated to be about 170 I_2/s from a window of channels on the basis of the results that $0.5\times 0.5 \times 0.3$ mm^3 size of the single crystal releases 6.96×10^{-11} mol of I_2 within the first 1 h. Once these interactions fade out with increasing I_2 extrusion, the delivery in the second stage is mainly governed by a free diffusion process, and a complete I_2 release from $\mathbf{1}'\supset 3I_2$ needs more than 11 days to attain the equilibrium state. However, I_2 release from zeolite 13X and activated carbon occurs within tens of minutes and then moves toward the equilibrium state (Figures S17−S19 (Supporting Information)). The two parameters, the maximum I_2 content and the rate, suggest that they may be due to a free diffusion process in the absence of well-defined host−guest interactions.

Taking the calculated density of I_2 in $\mathbf{1}'\supset 3I_2$ (2.48 g/cm^3) and the free volume of $\mathbf{1}'$ into account, the I_2 guests are expected to be confined and aligned in four close parallel chains in each channel and are surrounded by aromatic rings. The potential intermolecular interactions between I_2 and π-electron walls are important, as they allow a single path for I_2 molecules to access and be restricted within well-regulated narrow limits within the nanochannels, inducing n → σ^* charge transfer (CT).[19] Such an arrangement can result in cooperative electrical conductivity for $\mathbf{1}'\supset 3I_2$. Electrical conductivity measurements on single crystals of $\mathbf{1}'\supset 3I_2$ were performed by contacting gold electrodes with gold paint. $\sigma_{\parallel}$ and $\sigma_{\perp}$ values were found to be ca. 3.42×10^{-3} and 1.65×10^{-4} S/cm, respectively. This is significantly greater (440×) than the generally accepted value ($\sigma = 7.69 \times 10^{-6}$ S/cm) for I_2. An anisotropy factor ($\sigma_{\parallel}$, $\sigma_{\perp}$) of 21 implied an ordered arrangement mode of I_2 molecules and a preferred conductivity along I_2 chains in the channels.[17c] Such enhanced electronic properties are rarely reported in molecular-engineered crystals, and this demonstrates the cooperative properties based on host−guest interactions for porous MOF.[2]

In summary, we have constructed an unprecedented, highly stable MOF with rigid metal-organic pillars (Zn-lactate) connected by organic groups (pybz) forming the double walls. The square-shaped channels housed the DMF solvent of the reaction that can be exchanged for methanol and removed while retaining complete crystallinity. The activated empty phase has excellent and promising I_2 affinity, and it can be slowly delivered to ethanol controllably. Donor−acceptor (I_2−π-electron of the surface of the walls) interaction resulted in cooperative anisotropic electrical conductivity. Our results further support the idea that judiciously assembling MOFs with predesigned regular and suitable pores can find more applications in the encapsulation of functional substances to achieve novel oriented properties.[20]

Acknowledgment. This work was supported by the NSFC (No. 20871034), the NSFGX (No. 00832001Z), the Program for New Century Excellent Talents in University of the Ministry of Education China (NCET-07-217), the Project of Ten, Hundred, Thousand Distinguished Talents in New Century of Guangxi (No. 2006201), the GKN (Grant 0630006-5D) and the CNRS.

Supporting Information Available: Tables, figures, text, and CIF files giving details of syntheses, crystal data, and IR, PXRD, and additional UV/vis spectral data. This material is available free of charge via the Internet at http://pubs.acs.org.

References

(1) (a) Yaghi, O. M.; Furukawa, H. *J. Am. Chem. Soc.* **2009**, *131*, 8875–8883. (b) Czaja, A. U.; Trukhan, N.; Müller, U. *Chem. Soc. Rev.* **2009**, *38*, 1284–1293. (c) Li, J.-R.; Kuppler, R. J.; Zhou, H.-C. *Chem. Soc. Rev.* **2009**, *38*, 1477–1504.
(2) Batten, S. R.; Neville, S. M.; Turner, D. R. *Coordination Polymers Design, Analysis and Application*; The Royal Society of Chemistry: London, 2009.
(3) (a) Kurmoo, M. *Chem. Soc. Rev.* **2009**, *38*, 1353–1379. (b) Tranchemontagne, D. J.; Mendoza-Cortés, J. L.; O'Keeffe, M.; Yaghi, O. M. *Chem. Soc. Rev.* **2009**, *38*, 1257–1283.
(4) (a) Horcajada, P.; Serre, C.; Maurin, G.; Ramsahye, N. A.; Balas, F.; Vallet-Regí, M.; Sebban, M.; Taulelle, F.; Férey, G. *J. Am. Chem. Soc.* **2008**, *130*, 6774–6780. (b) Taylor-Pashow, K. M. L.; Rocca, J. D.; Xie, Z.-G.; Tran, S.; Lin, W.-B. *J. Am. Chem. Soc.* **2009**, *131*, 14261–14263.
(5) (a) Fang, Q.-R.; Zhu, G.-S.; Jin, Z.; Ji, Y.-Y.; Ye, J.-W.; Xue, M.; Yang, H.; Wang, Y.; Qiu, S.-L. *Angew. Chem., Int. Ed.* **2007**, *46*, 6638–6642. (b) Chae, H. K.; Siberio-Pérez, D. Y.; Kim, J.; Go, Y.; Eddaoudi, M.; Matzger, A. J.; O'Keeffe, M.; Yaghi, O. M. *Nature* **2004**, *427*, 523–527.
(6) (a) Dong, Y.-B.; Wang, P.; Ma, J.-P.; Zhao, X.-X.; Wang, H.-Y.; Tang, B.; Huang, R.-Q. *J. Am. Chem. Soc.* **2007**, *129*, 4872–4873. (b) Zhao, B.; Chen, X.-Y.; Cheng, P.; Liao, D.-Z.; Yan, S.-P.; Jiang, Z.-H. *J. Am. Chem. Soc.* **2004**, *126*, 15394–15395.
(7) Nakabayashi, K.; Kawano, M.; Yoshizawa, M.; Ohkoshi, S.; Fujita, M. *J. Am. Chem. Soc.* **2004**, *126*, 16694–16695.
(8) Lan, A.-J.; Li, K.-H.; Wu, H.-H.; Olson, D. H.; Emge, T. J.; Ki, W.; Hong, M. C.; Li, J. *Angew. Chem., Int. Ed.* **2009**, *48*, 2334–2339.
(9) Crystal data for **1**, tetragonal, $P42_1c$, $a = b = 24.886(1)$ Å, $c = 15.174(2)$ Å, $V = 9398(1)$ Å^3, $T = 173(2)$ K, $Z = 8$, $D_c = 1.345$ g cm^{-3}, final R1 = 0.0468 ($I > 2\sigma$), wR2 = 0.1437 (all data), $S = 1.138$. Crystal data for $\mathbf{1}'$: tetragonal, $P\bar{4}c2$, $a = b = 17.678(1)$ Å, $c = 15.133(2)$ Å, $V = 4729$ (1) Å^3, $Z = 4$, $D_c = 1.080$ g cm^{-3}, final R1 = 0.0422 ($I > 2\sigma$), wR2 = 0.1455 (all data), $S = 1.125$.
(10) Spek, A. L. PLATON, A Multipurpose Crystallographic Tool; Utrecht University, Utrecht, The Netherlands, 2003.
(11) Zeng, M.-H.; Feng, X.-L.; Zhang, W.-X.; Chen, X.-M. *Dalton Trans.* **2006**, 5294–5303.
(12) (a) Zeng, M.-H.; Hu, S.; Chen, Q.; Xie, G.; Shuai, Q.; Gao, S.-L.; Tang, L.-Y. *Inorg. Chem.* **2009**, *48*, 7070–7079. (b) Pan, L.; Parker, B.; Huang, X.-Y.; Olson, D. H.; Lee, J. Y.; Li, J. *J. Am. Chem. Soc.* **2006**, *128*, 4180–4181.
(13) Ouellette, W. A.; Prosvirin,; Whitenack, V. K.; Dunbar, K. R.; Zubieta, J. *Angew. Chem., Int. Ed.* **2009**, *48*, 2140–2144.
(14) Chester, A. W.; Clement, P.; Han, S. U.S. Patent 6,136,291A, 2000.
(15) (a) Kitagawa, S.; Matsuda, R. *Coord. Chem. Rev.* **2007**, *251*, 2490–2509. (b) Hu, S.; He, K.-H.; Zeng, M.-H.; Zou, H.-H.; Jiang, Y.-M. *Inorg. Chem.* **2008**, *47*, 5218–5224. (c) Zhang, J.-P.; Chen, X.-M. *J. Am. Chem. Soc.* **2009**, *131*, 5516–5521.
(16) Murthi, M.; Snurr, R. Q. *Langmuir* **2004**, *20*, 2489–2497.
(17) (a) Görbitz, C. H.; Nilsen, M.; Szeto, K.; Tangen, L. W. *Chem. Commun.* **2005**, 4288–4290. (b) Mohanambe, L.; Vasudevan, S. *Inorg. Chem.* **2004**, *43*, 6421–6425. (c) Hertzsch, T.; Budde, F.; Weber, E.; Hülliger, J. *Angew. Chem., Int. Ed.* **2002**, *41*, 2281–2284.
(18) (a) Wang, Z.-M.; Zhang, Y.-J.; Liu, T.; Kurmoo, M.; Gao, S. *Adv. Funct. Mater.* **2007**, *17*, 1523–1536. (b) Wang, Z.-M.; Zhang, B.; Fujiwara, H.; Kobayashi, H.; Kurmoo, M. *Chem. Commun.* **2004**, 416–417. (c) Choi, H. J.; Suh, M. P. *J. Am. Chem. Soc.* **2004**, *126*, 15844–15851. (d) Lu, J. Y.; Babb, A. M. *Chem. Commun.* **2003**, 1346–1347. (e) Abrahams, B. F.; Moylan, M.; Orchard, S. D.; Robson, R. *Angew. Chem., Int. Ed.* **2003**, *42*, 1848–1851.
(19) DeBoer, G.; Burnett, J. W.; Young, M. A. *Chem. Phys. Lett.* **1996**, *259*, 368–374.
(20) Suh, M. P.; Cheon, Y. E.; Lee, E. Y. *Coord. Chem. Rev.* **2008**, *252*, 1007–1026.

JA908293N